Available online at www.sciencedirect.com

ScienceDirect

Transportation Research Procedia 45 (2020) 898–905

Transportation Research Procedia

www.elsevier.com/locate/procedia

AIIT 2nd International Congress on Transport Infrastructure and Systems in a changing world (TIS ROMA 2019), 23rd-24th September 2019, Rome, Italy

Analysis of Road Safety Speed from Floating Car Data

Chiara Colombaroni[a], Gaetano Fusco[a]*, Natalia Isaenko[a]

[a]*Sapienza University of Rome, Via Eudossiana 18, Rome 00184, Italy*

Abstract

Intelligent Transportation Systems aims at improving efficiency and safety of the transportation system by acting either on vehicle performances or assisting the driver with information on vehicle and traffic status. Although digital road graphs are available to derive quantitative parameters that describe the road geometry, the information provided usually includes speed limits and repetition of road signs. On the other hand, a huge amount of data is available on individual vehicle speeds and trajectories collected as Floating Car Data (FCD) but they are not combined with road parameters to derive information on how drivers perceive the infrastructure and behave when traveling on it. In the paper, a methodology is presented to evaluate the consistency between drivers' behavior and a theoretical safety speed determined from road geometry. The azimuth profile is progressively built for a road layout, based on the geometry described by a digital graph. Consecutive elements with the constant azimuth variation are identified as circular curves and their radii are computed by circle fitting. The safety speed with respect to longitudinal stability is estimated. The obtained safety speed is then compared to the distribution of speeds observed from about 200 million FCD collected on the regional road network of Latium. The obtained results permit to individuate critical points of the network in terms of road safety.

Keywords: Road Safety; Floating Car Data; Road geometry; Drivers Behavior

1. Introduction

Intelligent Transportation Systems aim at improving efficiency and safety of the transportation system by acting either on vehicle performances or assisting the driver with information on vehicle and traffic status (Fusco et al., 2017). Although digital road graphs are available to derive quantitative parameters that describe the road geometry,

* Corresponding author. Tel.: +39-06-44585-128.
E-mail address: gaetano.fusco@uniroma1.it

10.1016/j.trpro.2020.02.078

information provided usually includes speed limits and repetition of road signs. In order to mitigate accident risk connected with high-speed traveler behavior curves have restricted values for the posted speed limit. However, many studies have shown that quite a few drivers comply with the suggested speed values (Donald, 1997). Among these studies, it was found that the difference between the observed operating speed and the posted speed exceeded 20 km/h (Chowdhury et al., 1998) and that only between 23 and 64 percent of drivers operated at or below the posted speed limit (Fitzpatrick et al., 2003). An experimental study (Charlton, 2004) highlighted that only in case of severe curves with reduced radii values operating speed was reduced by introducing different warning measures.

On the other hand, a huge amount of data on individual vehicle speeds and trajectories collected as Floating Car Data (FCD) enabled many studies using trajectory data in travel behavior, travel pattern, while urban planning covers applications in traffic management schemes and commercial services (Kong et al., 2018). Individual FCD enable adopting different spatial levels of aggregation in order to extract knowledge about traffic dynamics (Isaenko et al., 2017). Applications concerning traffic safety include estimation of free flow speed (Diependaele et al., 2016), retrieve of road geometry parameters (Neuhold et al., 2017), and use of real-time collected data for safety monitoring and accident prediction (Shi and Abdel-Aty, 2015).

This paper addresses using FCD to derive information on how drivers perceive the infrastructure and behave when traveling on it while a digital road graph is used in order to obtain road parameters. From the road safety perspective, it is desirable that the running speed of a large proportion of drivers be lower than the design speed. Experience indicates that deviations from this desired goal are most evident on sharper horizontal curves. In particular, curves with low design speeds (relative to driver expectation) are frequently overdriven and may have higher crash frequencies (AASHTO, 2011). Consistently with this remark, the paper focuses on the safety conditions against skidding and vehicle rollout in curves and neglects the other even relevant factors that affect the road safety.

In order to analyze the level of consistency between travelers' behaviors and safety conditions imposed by road geometry, this study follows the methodological framework reported in Fig. 1. Two types of analysis are conducted: the first analysis concerns the identification of homogenous road sections and computation of safety speeds; the second analysis concerns the frequency distributions of available floating car data on different homogenous sections of the road.

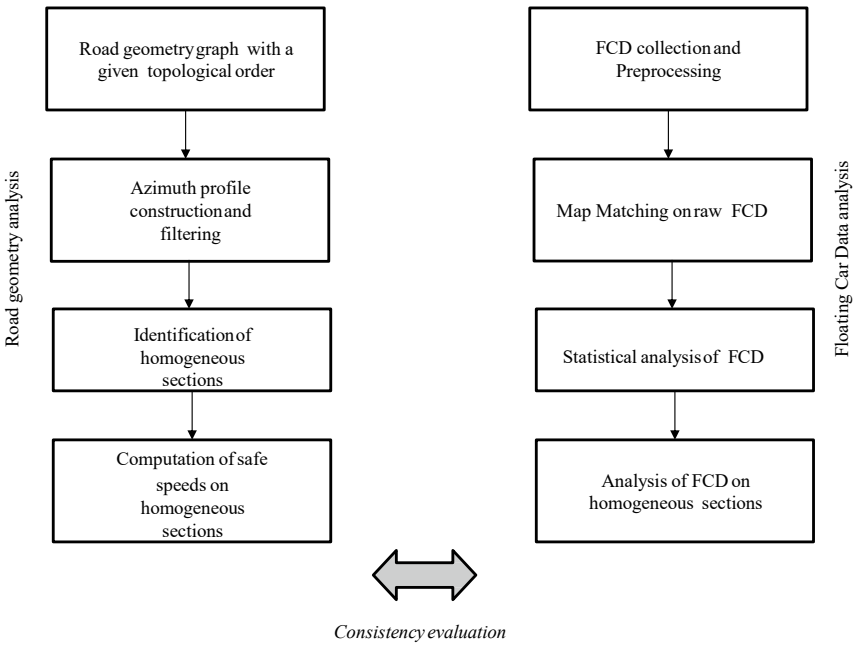

Fig. 1 Analysis of road geometry and floating car data

2. Road geometry analysis

Road geometry analysis aims to identify homogenous sections on the road and individuate the corresponding speeds that comply with longitudinal stability conditions. Homogenous sections are either straight segments or curves where the relative safety speeds are defined by stability conditions on curves.

2.1. Azimuth profile construction and identification of homogenous sections

In order to identify homogeneous sections, the azimuth profile is computed for the whole longitudinal profile of the road. Road geometry characteristics are derived from a digital road graph as a sequence of links, which can have both straight or curve geometry. Thus, in order to obtain a continuous azimuth profile for a road layout, a given topological order on the graph needs to be followed when computing azimuth values. In such a way, azimuth values vary linearly on circular curve segments and maintain constant values on straight segments. Commercial digital road graphs are highly detailed, and the road geometry is described precisely with reference to the road axis or even for each lane. Both curves and straight segments are normally represented by polylines, that are connected series of line segments. Since curve sections are represented as very dense sequences of straight segments with different angles and even relatively straight sections are still represented as a sequence of straight segments with slightly different angles, the resulting azimuth profile is noisy, as depicted in Fig. 2-a. In this figure, the link is divided into segments of 0.5 m length and the azimuth value is computed for all segments.

To smooth the noise in the data a digital filter is applied (Savitzky and Golay, 1964) that uses least squares calculations in order to fit a low-degree polynomial on observed data subsets. Once the smoothed profile is obtained, a heuristic search for local maxima and minima is performed to determine homogenous sections on the road. This searching method progressively scans the data and identifies a local maximum in case a point has a maximal value and is preceded by a value lower than a given threshold. Fig. 2-b reports the filtered azimuth profile for the 13km long Cassia Veientana road and the corresponding filtered azimuth profile. In the figure, the filter was fitted using 200 adjacent data points that correspond to 100 meters and polynomial order of 3. The blue points indicate the local minima and maxima individuated for the filtered profile by the heuristic search with a threshold of 2. The local maxima and minima points enable to divide the road into homogenous sections, which are either straight sections whose azimuth is almost constant and curve sections with variable azimuth. However, it is worth noticing that some homogenous section identified by the algorithm may have a very limited extension and therefore cannot be perceived by drivers as a proper section that requires a speed change. In the example reported in Fig. 2-b, the minimum length for the homogenous sections was set to 200 meters. Point 3 and point 14, indicated by red triangles, are two cases of homogenous sections having almost constant azimuth value and extension shorter 100 meters. In both cases, short homogenous sections were equally split between the two adjacent homogenous sections with variable azimuth values. In general, the sections with shorter extensions are merged into a unique section in case of a sequence of short segments or they are directly associated with longer segments if the short segments are adjacent to longer homogenous sections.

Once the homogenous sections are identified within a road profile, the corresponding safety speeds with respect to longitudinal stability need to be determined. On curve sections, the safety speed depends on the radius value. In order to fit a circular curve and estimate the corresponding radius the circle equation is written in the following form:

$$x^2 + y^2 + a_1 x + a_2 y + a_3 = 0 \tag{1}$$

$$a_1 x + a_2 y + a_3 = -(x^2 + y^2) \tag{2}$$

where x, y are the coordinates in the horizontal plane and a_1, a_2, a_3 are coefficients to determine.

Thereafter, the vector of coefficients **a** can be estimated by minimizing the squared difference between the curve and m known data points by solving the following equation:

$$\mathbf{Ca} = -\mathbf{B}, \text{ where } \mathbf{C} = \begin{bmatrix} x_1 & y_1 & 1 \\ x_2 & y_2 & 1 \\ x_m & y_m & 1 \end{bmatrix}, \mathbf{a} = \begin{bmatrix} a_1 \\ a_2 \\ a_3 \end{bmatrix}, \mathbf{B} = \begin{bmatrix} x_1^2 + y_1^2 \\ x_2^2 + y_2^2 \\ x_m^2 + y_m^2 \end{bmatrix} \tag{3}$$

Fig. 3-a reports a map with the homogenous curve sections individuated for Cassia Veientana road and the corresponding fitted circular curves with the radius values.

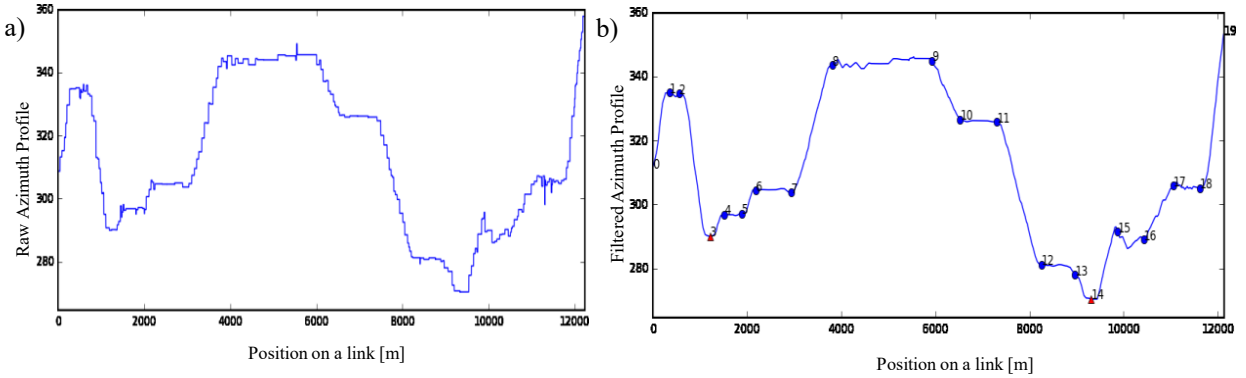

Fig. 2. (a) Raw azimuth profile with azimuth value computed every 0.5 m, (b) Filtered azimuth profile with identified homogenous sections.

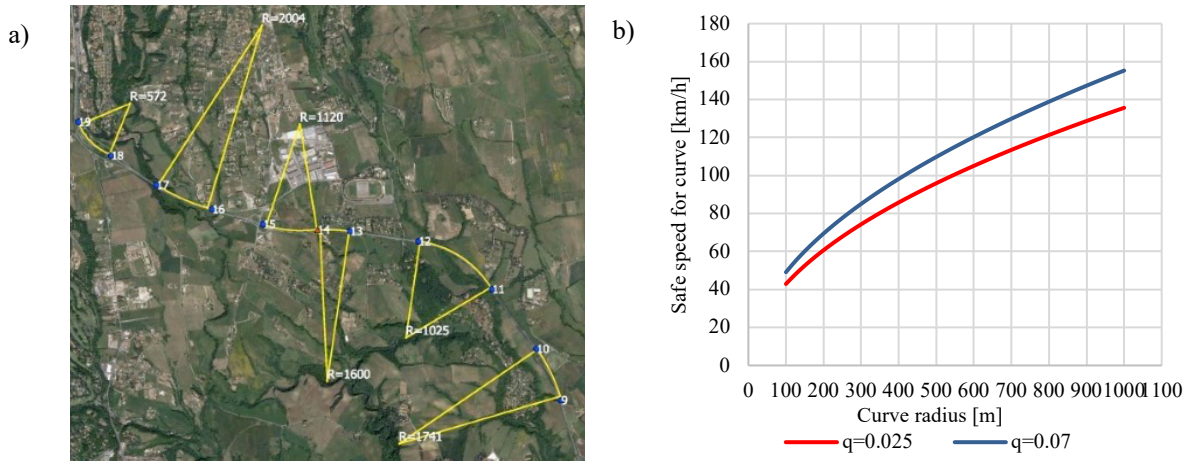

Fig. 3. (a) Radii of circular curves obtained after circle fitting on Cassia Veientana road, (b) Relationship between curve radius and safety speed according to longitudinal stability conditions on road curves for different values of the slope q assuming a side friction factor f_t=0.12.

2.2. Safety speed definition

For new road construction the road design legislation introduces a range of design speeds, which is the range of values defining road layout characteristics (MIT, 2001). The upper limit of this interval is the reference speed for the design of the least critical elements of the road, while the lower limit is meant as the reference speed for the design of the most critical elements.

In this study, it is assumed that the actual safety conditions on the existing roads can be assessed by using the design speed values. For circular curves, which usually are the most critical elements of the road layout, the safety condition for skidding and vehicle rollover is determined by the geometric characteristics of the curve. The fundamental relationship between speed and radius is used in design to express the design speed in terms of superelevation and side friction factor:

$$V_l = \sqrt{127(q + f_t)R} \tag{4}$$

where:

$q = i / 100$ is the superelevation

R is the radius in meters

f_t is the side friction factor, which is itself a function of the vehicle's speed V.

For most historical roads, the superelevation is not known from the characteristics of the graph and can be assumed by conversely using the prescriptions of the regulations for road design. These establish minimum and maximum

values of the superelevation according to the curve radius and for different values of the design speed, described in parametric form.

According to Italian regulations, the superelevation of main rural roads varies between 2.5% (minimum) for larger curve radii and 7% (maximum) for smaller curve radii. For curves with a design speed of 100 km/h and radii lower than 437m, the superelevation is 7%; for radii greater than 2,187m it is 2.5%. For intermediate values, the superelevation is determined based a non-linear relationship. Since on the existing roads studied in this analysis the real value of the superelevation is not known from the available data, two relations $V = V(R)$ are derived for the extreme values of the superelevation, that are 2.5% and 7%, in order to describe the whole definition range. Assuming a constant value for the side friction factor, the safety speeds against skidding and vehicle rollover conditions can be computed for both the maximum and minimum superelevation values in a closed form. In this analysis, the value of side friction factor f_t =0.12 is used that corresponds to the usual maximum posted speed on the rural highways under study (90 km/h). Hence, the following equations are obtained for minimum and maximum speeds.

$$V_{l,\min} = 4.29\sqrt{R} \text{ for } q=0.025;\ V_{l,\max} = 4.91\sqrt{R} \text{ for } q=0.07 \tag{5}$$

The two corresponding curves are shown in Fig. 3-b. Lacking any information on the actual superelevation, the average value of the two speeds defined above is adopted:

$$V_l = 0.5(V_{l,\min} + V_{l,\max}) \tag{6}$$

3. Floating Car Data analysis

Floating Car Data are obtained from a fleet of 30,000 vehicles equipped with a GPS device that provides the position and instantaneous speed of the vehicles, measured every 30s, for one year. Differently to traditional sensors at fixed monitoring stations, FCD have pervasive character both in time and space and can theoretically provide information at any point of the network. Every data point reports the individual position and speed, the state of the engine (turned on, turned off, in motion), the traveled distance from the previous measurement, the direction of motion, and the quality of GPS signal (depending on the number of satellite signals received). Before using the dataset, a data cleaning operation was performed to eliminate data having poor GPS signal quality (determined by the number of visible satellites), inconsistent data with the sequence of engine codes, and those with too short travelled distances. Further details can be found in Fusco et al., 2018.

The data used for transportation-oriented applications need to be referred to the specific elements of the transportation network by a map matching algorithm. In order to associate data points to the most likely links of the graph the algorithm takes into account the respective directions of the motion and the road links. Fig. 4-a reports an example of application of a map matching algorithm. The green elements represent unmatched data, the pink elements denote the matched data, and the arrows indicate the direction of the motion.

The information provided by FCD is collected only by a sample of vehicles floating in the total stream. Thus, these data provide ubiquitous but partial information for what it concerns traffic state estimation. However, statistical analysis involving large datasets provides significant insights on driver behavior. In order to address the consistency between travelers' behavior and safety conditions, the data matched on the road graph need to be furtherly aggregated. For what it concerns spatial aggregation, a high granularity is used in order to reveal specific unsafe points or segments on the network where point speed assumes high values with respect to the estimated safety speed. Fig. 4-b illustrates average values of the individual FCD with spatial aggregation of 20 meters.

Operating speed of a road is traditionally defined as 85th percentile of the distribution of individual vehicles traveling under free-flow conditions. Operating speed is thus determined by drivers' behavior and must be coherent with the speed determined by safety conditions. Naturally, the distribution of the observed individual speeds is variable along the road segment and depends on many exogenous factors, including weather and visibility conditions. The time of the day is also a very important issue that affects the distribution of the observed data and has to be taken into account to identify a suitable time aggregation level. Since the exact traffic state is not known in advance and the individual speeds distribution is unavoidably affected by traffic congestion or more in general by traffic states where conditioning between drivers takes place, it is necessary to use high percentiles of the observed distribution in order to address the operating speed. For example, the speed distribution during the night is expected to have a larger variance, which is another threating point for safety conditions on the road network.

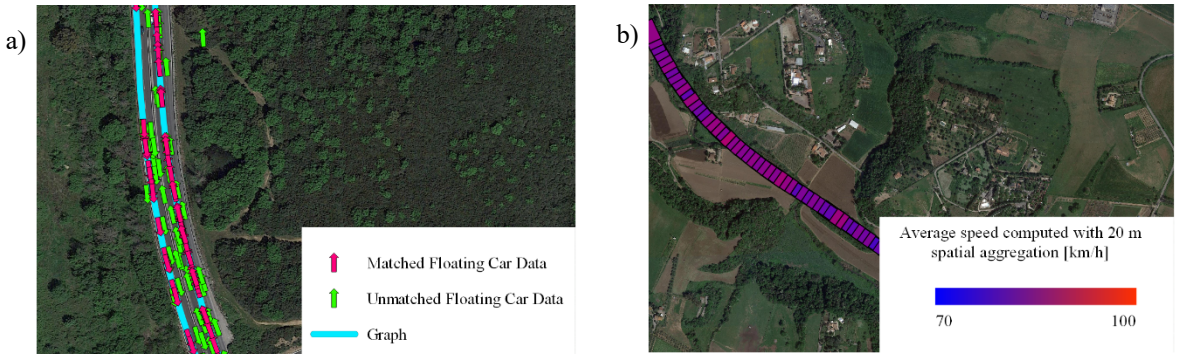

Fig. 4. (a) Example of application of a map matching algorithm to individual Floating Car Data; (b) Example of spatial aggregation of 20 meters adopted to obtain average speed values.

4. Application and results

The described procedure of consistency evaluation takes into account the safety speeds derived from road geometry reconstruction and the observed speeds provided by individual FCD. The analysis, conducted for ASTRAL, Road Agency of Latium Region, concerns 11 regional roads: SR 630 Ausonia, SR 6 Casilina, SR 2 Cassia, SR 213 Flacca, SR 3 Flaminia, SR 156 Monti Lepini, SR 207 Nettunense, SR 148 Pontina, SR 578 Salto Cicolana, SR 296 della Scafa and SR 5 Tiburtina.

A highly detailed digital graph with average link length of 200 meters ss used to derive the azimuth profile, compute circular curve fitting, and determine radii values. The minimal length for the homogenous sections is set to 200 meters; shorter sections are merged according to the criterion explained in Subsection 2.1. For each road, a Savitzky–Golay filter is fitted using 200-300 azimuth points, corresponding to 100-150 meters, and polynomial order from 3 to 7 in order to obtain a smoothed azimuth profile. Then, several high percentiles of the observed speeds distributions (85th, 90th and 95th) are compared with the safety speed. Fig. 5-a reports an example of the diagram for Cassia Veientana road. The safety speed is drawn in blue color: the continuous line identifies the homogeneous road sections whose safety speed is determined by the skidding and rollover conditions according to Equation (6); the dotted line denotes both straight and curve sections whose radii correspond to safety speed values greater than an upper limit, conventionally set to 140 km/h. In the same figure, the green line identifies the average speed while the lines in yellow, orange and red indicate the eighty-fifth, ninetieth and ninety-fifth percentile of the observed speed distributions (V_{85}, V_{90}, V_{95}).

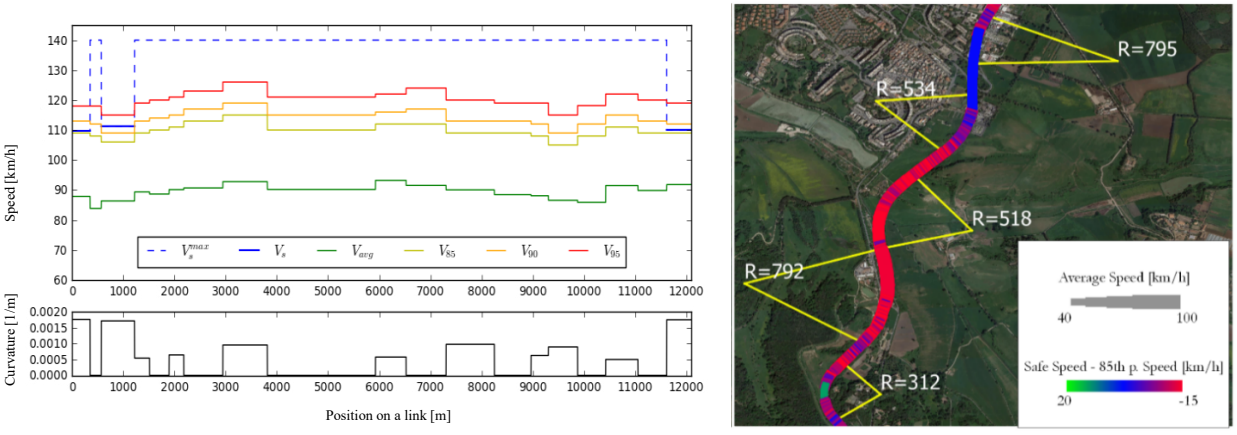

Fig. 5. (a) Safety speed and observed speed for Cassia Veientana road diagram; (b) An example of map difference between safety speed and 85th percentile of the observed speeds distribution.

Table 1. Safety indicators computed on roads object of study

Road Name	Δ_{avg}	Δ^-_{avg}	$L^{\%}_{avg}$	$1/R^-_{avg}$	Δ_{85}	Δ^-_{85}	$L^{\%}_{85}$	$1/R^-_{85}$	Δ_{95}	Δ^-_{95}	$L^{\%}_{95}$	$1/R^-_{95}$
SR630 Ausonia	25.78	-10.15	2%	0.016	8.61	-16.06	3%	0.016	-2.31	-6.63	71%	0.001
SR6 Casilina	29.84	-7.08	5%	0.011	14.42	-10.19	13%	0.008	5.71	-10.84	27%	0.004
SR2 Cassia	21.45	-6.10	10%	0.008	6.32	-12.13	34%	0.003	-2.47	-15.05	58%	0.003
SR213 Flacca	27.25	-7.75	4%	0.007	10.92	-9.85	15%	0.004	-0.05	-10.60	55%	0.002
SR3 Flaminia	27.54	-13.31	13%	0.011	13.26	-17.96	22%	0.009	5.91	-19.39	31%	0.007
SR156 Monti Lepini	32.49	-3.61	0%	0.005	9.69	-4.60	18%	0.001	-1.17	-8.98	62%	0.001
SR207 Nettunense	45.86	-4.51	0%	0.012	26.66	-9.20	1%	0.010	18.61	-7.02	3%	0.007
SR148 Pontina	12.32	-3.91	19%	0.000	-9.21	-14.97	74%	0.000	-20.46	-22.03	95%	0.000
SR578 Salto Cicolana	10.05	-4.83	24%	0.003	-10.30	-16.57	73%	0.002	-20.90	-26.17	78%	0.002
SR5 Tiburtina.	27.30	-6.87	14%	0.013	13.35	-10.11	27%	0.010	6.13	-11.89	42%	0.007

The analysis highlights three potentially critical sections of the road where a significant fraction of drivers exceeds the safety speed: respectively, the 10% of drivers for the initial and the final sections, and the 5% for the section around the point 1000m. On all other sections, safety speeds against skidding and rollover are higher than the conventional upper value and are not critical with respect to that condition.

The differences between the observed speed and safety speed are represented also on a thematic map for every road under analysis. The points of the road with observed speed exceeding the safety speed are highlighted by red colors; when the differences between the 85th percentile of the observed speed and the safety speed are negative blue and green colors are used. This kind of map, reported as an example in Fig. 5-b, enables associating critical points of the roads with reference to the overall road geometry and external conditions. For example, on the Pontina road the observed speeds exceed the safety speeds on several consecutive curves with narrow radii; moreover, an in-depth analysis showed that the vertical alignment of the sections reduced the sight distance and therefore represented a threating point for the safety conditions.

In order to assess quantitatively the observed safety conditions several critical safety indices are introduced:

$$\Delta_* = \frac{\sum_{i=1}^{N}(V_s - V_*)L_i}{L_{tot}}$$ average difference between the safety speed and the chosen percentile of the observed speed (7)

$$\Delta_*^- = \frac{\sum_{i=1}^{N}(V_s - V_*)L_i}{L_{\Delta^-}}$$ average difference between the safety speed and the chosen percentile of the observed speed on the segments where observed speed exceeds the safety speed (8)

$$L_*^{\%} = \frac{\sum_{i=1}^{N^-} L_i}{L_{tot}}100\%$$ percentage extension of the segments over total length of the road, where the chosen percentile of the observed speed exceeds the safety speed (9)

$$1/R_* = \frac{\sum_{i=1}^{N^-} 1/R_i}{N^-}$$ average curvature of the circular segments, where the chosen percentile of the observed speed exceeds the safety speed (10)

where V_* is the observed * percentile speed (avg-average, 85, 95); L_i is the length of i-th segment; N is the total number of segments; N^- is the total number of segments whose observed speed exceeds the safety speed; R_i the value of the radius on circular segment i.

The critical safety indices, reported in Table 1, are computed for all roads, excluding SR 296 della Scafa, where the observed speeds are always lower than the safety speeds. An alarming user behavior is revealed on both the SR 148 Pontina and the SR 578 Salto Cicolana, where the average speed exceeds the safety speed for over 20% of the total length of the road. This result in both cases is due to a high average speed along the entire road layout. The 85th percentile speed for both roads is over 96 km/h. The 85th percentile speeds exceed the safety speeds on 22%, 27% and 34% of the entire road extension respectively on SR 3 Flaminia, on SR 5 Tiburtina and on SR 2 Cassia. High values of the average curvature of the sections where the average speed is higher than the safety speed highlight driving behavior inconsistency on many curve road elements.

In the cases of SR 213 Flacca and SR 6 Casilina, the extension where the 85th percentile speed exceeds the safety speed is around 14% of the total length of the roads. However, on both roads, a detailed examination of user behavior revealed several curves where the operating speed exceeds the safety speed by 20 km/h.

5. Conclusion

The objective of this study was to evaluate the consistency between drivers' behavior and safety speed against skedding and rollover conditions, depending on the horizontal alignment of the road. The proposed methodology was applied to 11 regional roads of Latium region in Italy to individuate roads with higher values of critical indices. Thereafter, the critical points within same road were thoroughly assessed by an in-depth analysis to identify the existence of other factors that affected the road safety, such as vertical alignment, sight distance, junctions, etcetera.

The analysis can be useful for several possible applications to historical roads whose design values are unknown: compare the posted speed limits applied in horizontal curves with the estimated safety speed and review them, if necessary and confirmed by the assessment of safety against other criteria; consider the need for further interventions other than the posted speed limits if they demonstrated to be breached by significant fractions of drivers; rank the regional roads with respect to the safety indices in order to plan a review of posted speed limits and other possible interventions aimed at increasing the road safety.

A natural extension of this analysis is to compare the estimated safety speed values with accident data to verify which percentile is significantly correlated with the actual accident occurrences and to adjust the hypothesized values of the parameters used to determine the safety speed, such as side friction and superelevation, to maximize the correlation with the accidence occurrence or with a more general indicator of potential accidents.

Future development of the proposed study concerns using actually travelled trajectories instead of the available commercial graph for computing the safety conditions. On this regard, the analysis of the distributions of FCD on the cross sections of the roads enables individuating the average traveled trajectory for different lanes and computing a bundle of most likely traveled trajectories corresponding speed profiles which can then be compared with the speed profiles imposed by safety conditions.

References

AASHTO, 2011. A policy on geometric design of highways and streets. American Association of State Highway and Transportation Officials. ISBN: 978-1-56051-508-1.

Charlton, S.G., 2004. Perceptual and attentional effects on drivers' speed selection at curves. Accid. Anal. Prev. 36, 877–884. https://doi.org/10.1016/j.aap.2003.09.003

Chowdhury, M.A., Warren, D.L., Bissel, H., Taori, S., 1998. Are the criteria for setting advisory speeds on curves still relevant? ITE J. (Institute Transp. Eng. 68, 32–45.

Diependaele, K., Riguelle, F., Temmerman, P., 2016. Speed Behavior Indicators Based on Floating Car Data: Results of a Pilot Study in Belgium, in: Transportation Research Procedia. https://doi.org/10.1016/j.trpro.2016.05.111

Donald, D., 1997. Be warned! A review of curve warning signs and curve advisory speeds, Research Report ARR.

Fitzpatrick, K., Carlson, P., Wooldridge, M.D., 2003. Design speed, operating speed, and posted speed limit practices. Transp. Res. Board 82nd Annu. Meet.

Fusco, G., Colombaroni, C., Isaenko, N., 2017. Dynamic traveler information systems. In: "Intelligent transport systems (ITS): Past, present and future directions", Fusco, G. (Ed.). Nova Science Publisher, New York. 265-314.

Fusco, G., Bracci, A., Caligiuri, T., Colombaroni, C., Isaenko, N., 2018. Experimental analyses and clustering of travel choice behaviours by floating car big data in a large urban area. IET Intell. Transp. Syst. 12, 270–278. https://doi.org/10.1049/iet-its.2018.0015

Isaenko, N., Colombaroni, C., Fusco, G., 2017. Traffic dynamics estimation by using raw floating car data, in: 5th IEEE International Conference on Models and Technologies for Intelligent Transportation Systems, MT-ITS 2017 - Proceedings. https://doi.org/10.1109/MTITS.2017.8005604

Kong, X., Member, S., Li, M., Ma, K.A.I., Tian, K., 2018. Big Trajectory Data : A Survey of Applications and Services. IEEE Access 6, 58295–58306. https://doi.org/10.1109/ACCESS.2018.2873779

Neuhold, R., Haberl, M., Fellendorf, M., Pucher, G., Dolancic, M., Rudigier, M., Pfister, J., 2017. Generating a lane-specific transportation network based on floating-car data, in: Advances in Intelligent Systems and Computing. https://doi.org/10.1007/978-3-319-41682-3_84

Savitzky, A., Golay, M.J.E., 1964. Smoothing and Differentiation of Data by Simplified Least Squares Procedures. Anal. Chem. 36, 1627–1639. https://doi.org/10.1021/ac60214a047

Shi, Q., Abdel-Aty, M., 2015. Big Data applications in real-time traffic operation and safety monitoring and improvement on urban expressways. https://doi.org/10.1016/j.trc.2015.02.022